

A CRYSTALLOGRAPHIC STUDY OF SEMICONDUCTOR-METAL TRANSITIONS IN PURE AND V-DOPED Ti_2O_3

A. M. SHAIKH AND M. A. VISWAMITRA

Department of Physics

AND

C. N. R. RAO

Solid State and Structural Chemistry Unit, Indian Institute of Science, Bangalore 560 012, India

ABSTRACT

Variations of lattice dimensions, Ti-Ti distances and other structural parameters of Ti_2O_3 with temperature and with V-doping are reported. The results are consistent with the band crossing mechanism of the semiconductor-metal transition.

Ti_2O_3 undergoes a semiconductor-metal transition around 400° K without any accompanying change in crystal symmetry^{1,2}. The transition is, however, accompanied by a change in the c/a ratio. The transition is considered to be due to the crossing of a_1 and e_π bands with increase in temperature³. All the recent studies on the Ti_2O_3 transition are in conformity with this mechanism. According to this mechanism, the Ti-Ti distance along the three-fold axis should increase with

entirely in agreement with our results⁸ in that both the studies show the expected variations in Ti-Ti distances and other structural parameters with temperature. In this communication, we report the results of our detailed crystallographic studies on the V_2O_3 -doped Ti_2O_3 system. We consider these studies to be important in understanding the mechanism of the semiconductor-metal transition in Ti_2O_3 and the mode of action of the V^{3+} impurity.

TABLE I
Lattice parameters and structural data of V_2O_3 -doped Ti_2O_3

	Ti_2O_3	0.5% V_2O_3	2.0% V_2O_3	4% V_2O_3	10% V_2O_3	H.T. Ti_2O_3 (580° K)
a Å	5.431 (1)	5.431 (1)	5.439 (1)	5.451 (4)	5.473 (1)	5.478 (2)
a deg	56.71 (1)	56.627 (1)	56.37 (1)	56.07 (2)	55.57 (1)	55.84 (1)
a_{hex} Å	5.159 (2)	5.155 (2)	5.138 (1)	5.125 (3)	5.162 (1)	5.129 (2)
c_{hex} Å	13.625 (2)	13.629 (2)	13.677 (3)	13.735 (3)	13.840 (3)	13.823 (2)
c/a	2.641	2.644	2.662	2.680	2.713	2.695
Bond Length Å						
$\text{M}_1\text{-M}_2$	2.582 (1)	2.584 (0)	2.602 (0)	2.628 (0)	2.658 (0)	2.657 (0)
$\text{M}_1\text{-M}_3$	2.994 (0)	2.989 (0)	2.982 (0)	2.976 (0)	2.968 (0)	2.982 (0)
$\text{M}_1\text{-O}_1$	2.067 (1)	2.061 (2)	2.067 (1)	2.070 (2)	2.072 (1)	2.079 (1)
$\text{M}_1\text{-O}_5$	2.027 (0)	2.027 (1)	2.019 (0)	2.017 (1)	2.012 (1)	2.019 (1)
$\text{O}_1\text{-O}_2$	2.796 (1)	2.787 (2)	2.782 (1)	2.769 (2)	2.753 (1)	2.769 (1)
$\text{O}_4\text{-O}_5$	3.073 (1)	3.074 (1)	3.060 (1)	3.056 (1)	3.048 (1)	3.062 (1)
$\text{O}_1\text{-O}_4$	2.792 (1)	2.787 (2)	2.791 (1)	2.801 (2)	2.805 (1)	2.811 (2)
$\text{O}_1\text{-O}_1$	2.882 (2)	2.882 (3)	2.881 (2)	2.894 (3)	2.899 (2)	2.904 (2)

temperature, while the opposite would be true for the Ti-Ti distance in the basal plane. Doping of Ti_2O_3 by V_2O_3 progressively reduces the magnitude of the conductivity jump, until at 10% V_2O_3 , the material is metallic⁴; the lattice parameters of 10% V_2O_3 -doped sample are reported to be close to those of the high temperature metallic phase of Ti_2O_3 ^{5,6}. We have been carrying out detailed crystallographic studies of pure Ti_2O_3 and also of Ti_2O_3 doped with V_2O_3 for the past some time. We have just noticed a publication of Rice and Robinson⁷, on the temperature-dependent structural changes in pure Ti_2O_3 . The results of these workers are

Single crystals of Ti_2O_3 and V_2O_3 -doped Ti_2O_3 were mounted on the goniometer head of an Enraf-Nonius CAD-4 diffractometer. A high temperature attachment built locally was used for the study of Ti_2O_3 ⁹. Lorentz polarisation and absorption corrections were applied and the structures refined by least-square treatment.

Variations of the lattice parameters of Ti_2O_3 with temperature and also with the incorporation of V_2O_3 are shown in Fig. 1. We see from the figure that the lattice parameter variations in the two cases are not exactly identical. Thus, the unit cell volume of Ti_2O_3 increases with tempera-

ture (just as the c/a ratio), in contrast to the earlier report in the literature¹⁰. The present observation of volume increase during the transition seems to explain the absence of pressure effect on the Ti_2O_3 transition¹¹. With the incorporation of

V_2O_3 , however, the unit cell volume decreases. This may be because, a_{hex} as well as a vary more steeply with $\% \text{V}_2\text{O}_3$ than with increasing temperature.

Lattice dimensions as well as the detailed structural parameters of V_2O_3 -doped Ti_2O_3 samples are given in Table I; for the purpose of comparison, the data on the high temperature phase of Ti_2O_3 are also given. In the crystal structure of Ti_2O_3 which is isomorphous with corundum structure, a given Ti atom, M_1 , has four near Ti neighbours: one M_2 , sharing a face of the oxygen octahedron, and three M_3 , sharing edges of the octahedron¹². We see from Table I that incorporation of V_2O_3 results in an increase in the M_1-M_2 distance across the shared octahedral face (just as with increase in temperature) from 2.582 Å in Ti_2O_3 to 2.658 Å in 10% V_2O_3 doped Ti_2O_3 (Fig. 2). This increase in M_1-M_2 is accompanied

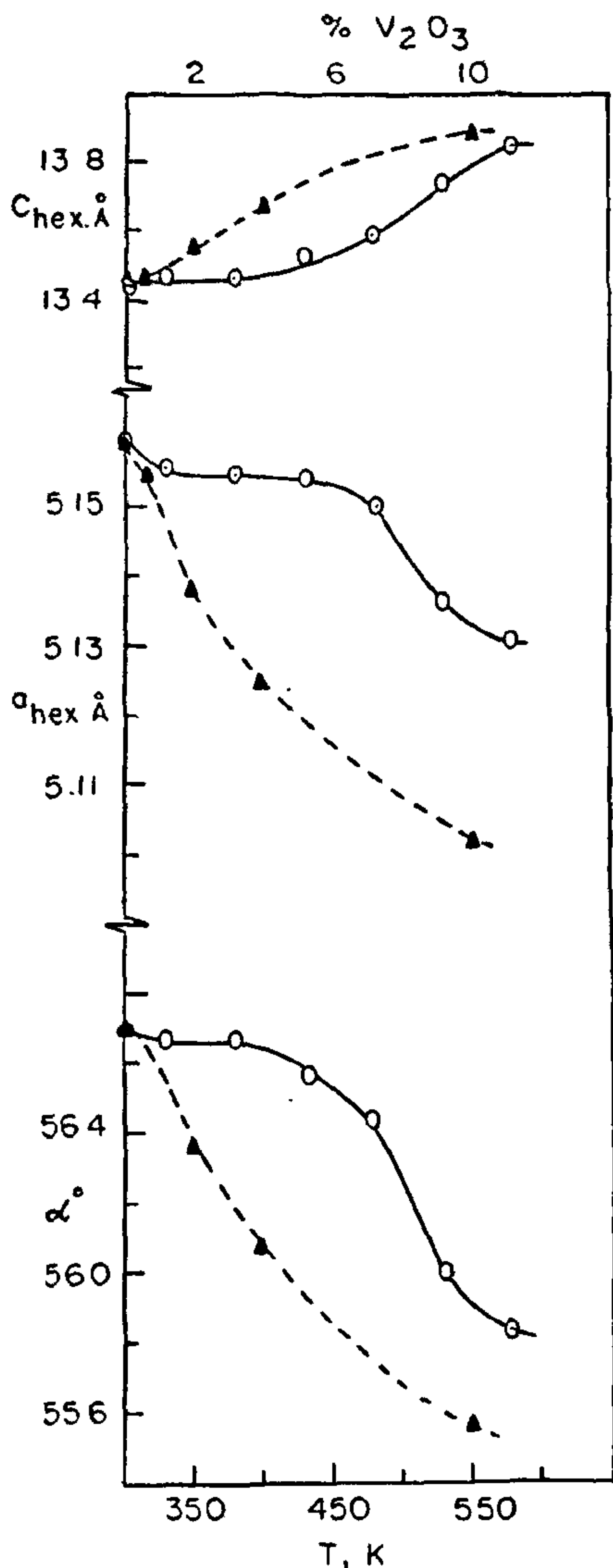


FIG. 1. Variation of lattice parameters of Ti_2O_3 with temperature (full lines) and with incorporation of V_2O_3 (broken lines) at 298° K.

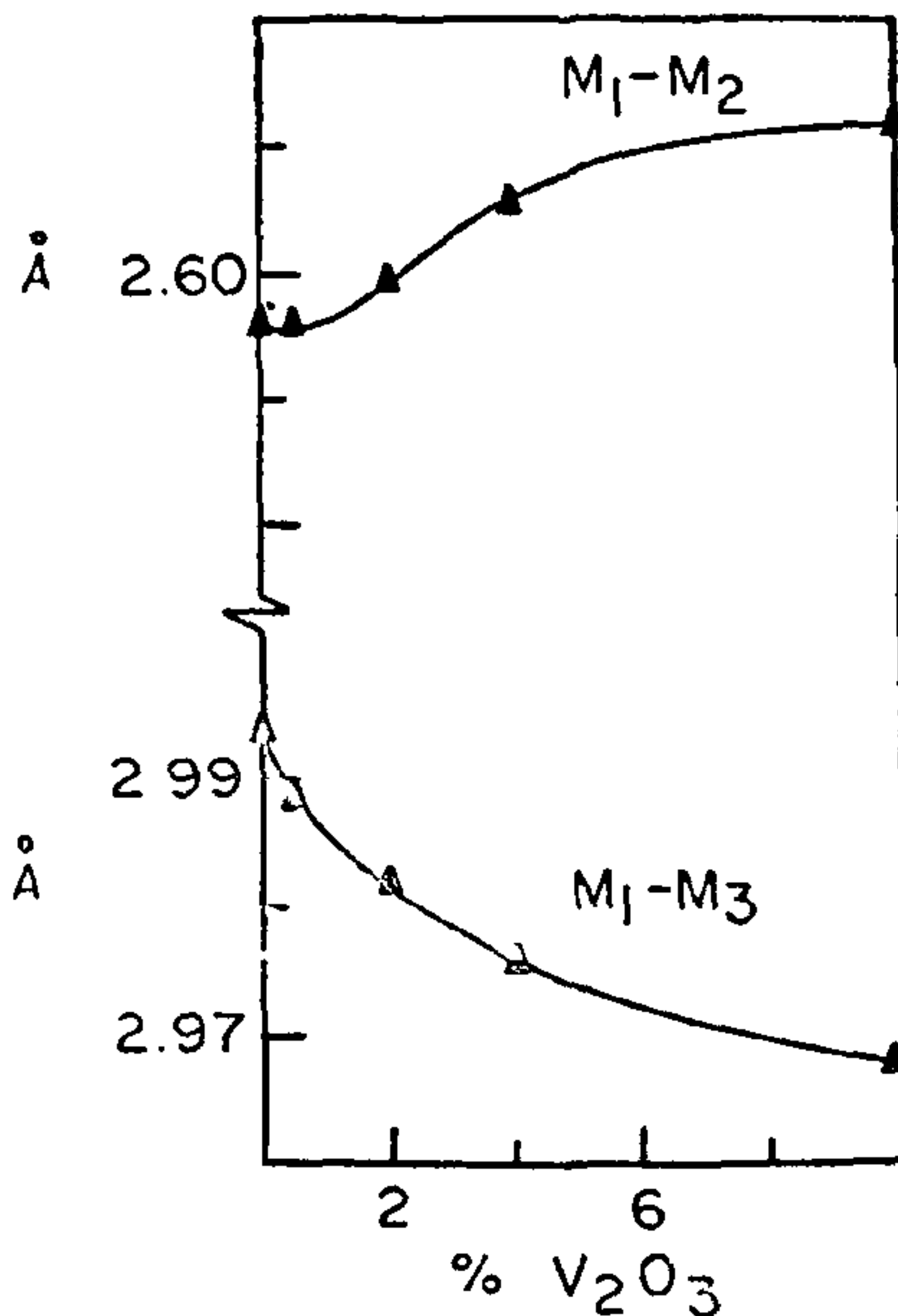


FIG. 2. Variation of Ti-Ti distances in Ti_2O_3 with incorporation of V_2O_3 at 298° K.

by an increase in the c -parameter and in the distance of M_1 from the O_1-O_3 plane perpendicular to this axis. Doping with V_2O_3 also causes a decrease in the M_1-M_3 distance from 2.994 Å in pure Ti_2O_3 to 2.968 Å in 10% V_2O_3 -doped sample (Fig. 2); this decrease in the Ti-Ti distance in the basal plane is accompanied by a decrease in

the α parameter. The M-O distances vary only slightly, but we do notice a significant variation in the $M_1-O_1-M_2$ angle from 77.3° in pure Ti_2O_3 to 79.79° in the 10% V_2O_3 -doped sample. Other angles which show significant variations are: $O_1-M_1-O_2$ and $O_1-M_1-O_6$ (decrease), $O_1-M_1-O_5$ (increase). The distances from M_1 (as well as O_4) to the O_1-O_3 plane also increase with incorporation of V_2O_3 . Decrease in α_{hex} with % V_2O_3 is consistent with the reduction in the O_1-O_2 distance.

The Debye-Waller factor in pure Ti_2O_3 shows a marked increase in the temperature region of the transition. The Debye-Waller factor shows a similar variation with % V_2O_3 as well.

The results of the present study show that the electronic properties of V_2O_3 -doped Ti_2O_3 can be explained by the band broadening mechanism of Van Zandt, Honig and Goodenough³. More specifically, the present study confirms that the two narrow d -bands cross each other following variations in the crystallographic c/a ratio¹³.

One of us (AMS) thanks the Council of Scientific and Industrial Research, New Delhi, for the award of a research fellowship.

1. Mott, N. F., *Metal-Insulator Transitions*, Taylor and Francis, London, 1974.

2. Rao, C. N. R. and Subba Rao, G. V., *Transition Metal Oxides*, NSRDS-NBS, Monograph 49, National Bureau of Standards, Washington, D.C., 1974.
3. Van Zandt, L. L., Honig, J. M. and Goodenough, J. B., *J. Appl. Phys.*, 1968, **39**, 594.
4. Chandrashekhar, G. V., Choi, Q. W., Moyo, J. and Honig, J. M., *Mat. Res. Bull.*, 1970, **5**, 999.
5. Loehman, R. E., Rao, C. N. R. and Honig, J. M., *J. Phys. Chem.*, 1969, **73**, 1781.
6. Robinson, W. R., *J. Solid State Chem.*, 1974, **9**, 255.
7. Rice, C. E. and Robinson, W. R., *Mat. Res. Bull.*, 1976, **11**, 1355.
8. Shaikh, A. M., Verugheese, K. I., Viswamitra, M. A. and Rao, C. N. R., *Abstracts of the National Conference on Crystallography*, Madras, January 1977.
9. — and Viswamitra, M. A., *Ibid.*, Madras, January 1977.
10. Rao, C. N. R., Loehman, R. E. and Honig, J. M., *Phys. Lett.*, 1968, **27 A**, 271.
11. Viswanathan, B., Usha Devi, S. and Rao, C. N. R., *Pramāṇa*, 1973, **1**, 48.
12. Newnham, R. E. and de Haan, Y. M., *Z. Krist.*, 1962, **117**, 235.
13. Goodenough, J. B., *Proceedings of the 10th International Conference on the Physics of Semiconductors*, Cambridge, Mass., U.S.A., 1970, p. 304.

ONSET HEIGHT OF RANGE-SPREAD F OVER THE EQUATOR

R. G. RASTOGI

Physical Research Laboratory, Ahmedabad 380 009 (India)

ABSTRACT

It is shown that Range-Spread F over the dip equator is first generated in the region between the base of the F region and the normal E region height. Later intensification of spread F is due to the combined effect of upward drift of irregularity and downward movement of the F layer. Range-spread is suggested to be generated in regions of large plasma gradient which is present after sunset in 100–200 km range.

INTRODUCTION

SPREAD F is generally considered to be due to the existence of plasma irregularities within the F region. Equatorial spread F has been associated with post-sunset rapid rise of the F layer. A threshold height has been also suggested for the F layer to rise before spread F can be seen. The model suggested by Clemsha and Wright² (1966) assumes the presence of irregularities above a certain height which is seen as spread F once the F layer rises above them. Cohen and Bowles³ (1961) have described transequatorial VHF forward scatter propagation through spread F and they estimated the height of these irregularities to be at the bottom or below the F layer. Rastogi⁴ (1977)

has shown the existence of spread F simultaneously with high order multiple echoes from the normal F region and suggested that even at the times of strong spread F, the normal F region has smooth ionization variation with height and that the irregularities responsible for the spread F are below the F region. Normally during the spread F condition the normal F region trace is mixed up with the spread F echoes and the former is not discernible. In this short note are presented some ionograms taken at the equatorial station Huancayo during spread F conditions.

Chandra and Rastogi¹ (1972) have shown that the equatorial spread F is of two types, Range and Frequency type spread. The spread F configura-